Egyptian Informatics Journal 21 (2020) 37–49

Contents lists available at ScienceDirect

Egyptian Informatics Journal

journal homepage: www.sciencedirect.com

Noise robust Laws' filters based on fuzzy filters for texture classification

Sonali Dash [a,*], Manas Ranjan Senapati [b]

[a] Department of Electronics and Communication Engineering, Raghu Institute of Technology, Visakhapatnam 531162, Andhra Pradesh, India
[b] Department of Information Technology, Veer Surendra Sai University of Technology, Burla 768018, Odisha, India

ARTICLE INFO

Article history:
Received 20 May 2018
Revised 13 July 2019
Accepted 15 October 2019
Available online 3 November 2019

Keywords:
Fuzzy filter
Laws' mask
Texture classification
Texture features

ABSTRACT

Laws' mask method has achieved wide acceptance in texture analysis, however it is not robust to noise. Fuzzy filters are well known for denoising applications. This work proposes a noise-robust Laws' mask descriptor by integrating the exiting fuzzy filters with the traditional Laws' mask for the improvement of texture classification of noisy texture images. Images are corrupted by adding Gaussian noise of different values. These noisy images are transformed into fuzzy images through fuzzy filters of different windows. Then the texture features are extracted using Laws' mask descriptor. To investigate the proposed techniques two texture databases i.e. Brodatz and STex are used. The proposals are assessed by comparing the performance of the traditional Laws' mask descriptor alone and after combined with the fuzzy filters on noisy images. The k-Nearest Neighbor (k-NN) classifier is utilized in the classification task. Results indicate that the proposed approach delivers higher classification accuracy than the traditional Laws' mask method. Hence, validate that the suggested methods significantly improve the noised texture classification.

1. Introduction

The study of image texture is well suited for several difficult tasks in computer vision. Its numerous applications vary from object recognition to content-based image retrieval. In the 1970s, the first work in the texture classification is proposed by Haralick, which has been focused on the statistical analysis of images [1]. At the end of same decade 1979, Laws has proposed texture analysis using convolutions [2–3]. The main contribution of this approach is the filtering of images with specific masks created from the combination of one-dimensional Kernel vector in order to evaluate the texture properties. Originally, Laws has classified samples based on expected values of variance-like square measures of these convolutions and named as "texture energy measures". Later on, many researchers have used Laws' mask descriptor for medical image analysis [4–7]. In a view of extending the Laws' mask method to the frequency domain recently Dash et al. have recommended hybrid models of Laws' mask descriptor and achieved higher classification rates than the traditional Laws' mask method [8–9]. Dash et al. have also suggested an improvement in texture classification by integrating the bilateral filter with the original Laws' mask descriptor [10]. They have also recommended an improved colour texture classification by using homomorphic normalization and by extracting texture features through traditional texture analysis techniques such as Gray Level Co-occurrence Matrix (GLCM) and Laws' mask [11].

Noise reduction in images has been one of the common tasks in image processing. Fuzzy techniques have already been applied in several domains of image processing. Various fuzzy filters for noise reduction have been recommended in the literature [12–15]. Compare with the classical filter, Fuzzy filters provide better results in reducing noise in image processing tasks [16]. In 2003, Kwan has introduced seven fuzzy filters for noise reduction and achieved success in noise reduction in images [17]. Some authors have also used fuzzy theory for classification purpose [18–20]. Various researchers have extended the traditional Local binary pattern (LBP) descriptor to noise-robust descriptor with hybrid models [21–23]. The literature study has also revealed about some original fuzzy filters are combined with existing filters to reduce noise in images. For example, Biradar et al. have proposed triangular fuzzy filter with moving average center (TMAV) with wiener filter for

* Corresponding author.
E-mail address: sonali.isan@gmail.com (S. Dash).

Peer review under responsibility of Faculty of Computers and Information, Cairo University.

Production and hosting by Elsevier

https://doi.org/10.1016/j.eij.2019.10.003
1110-8665/

speckle noise reduction in images [24]. Santoso et al. have proposed fuzzy approaches by combining the existing fuzzy filters with Frost filter for speckle noise reduction. They have utilized the existing fuzzy filters such as, fuzzy filter with symmetrical triangular with median center (TMED), the fuzzy filter with asymmetrical triangular with median center (ATMED), the fuzzy filter with triangular function with moving average center (TMAV) and the fuzzy filter with asymmetrical triangular function with moving average center (ATMV) [25]. Russo and Ramponi have recommended a dual step fuzzy-ruled-based filter to detect and remove large amount of impulse noise. Harron et al. have reduced the noise to improve the classification using textural information [26]. They have used recursive least square filter for the reduction of noise [27]. Schulte et al. have proposed two step fuzzy filter for the reduction of impulse noise in colour images [28]. Mehra et al. have suggested denoising of images in wavelet domain by using fuzzy and wiener filter [29]. Bansal et al. have utilized thresholding technique for removing impulse noise through simplified fuzzy filter [30]. Toh and Isa have suggested a noise adaptive fuzzy switching median filter for removal of salt-and-pepper noise [31].

The literature study exposes that fuzzy filters in many forms have been applied in many diversified filed. However, the issues related to de-noising of noisy texture images are remained as a great challenge. In general, there are two types of noises like impulse (salt and pepper) noise, and random (or Gaussian) noise. Impulse noise is represented by noise density whereas random noise is expressed in terms of its mean and variance. For impulse noise, maximum portion of an original image remains unchanged, and the image is distinguished by some corrupted samples, which differ intensely. In comparison to impulse noise, random noise is more challenging type of noise. Hence, it is an essential task to reduce the random noise effectively in images. In literature many types of linear and nonlinear filtering techniques have been suggested for noise removal for example median (MED) filter and moving average (MAV) filter. Median filter performs in an average manner to filter the random noise. A nonlinear filter named as moving average filter performs well in removing random noise but neither they can supress impulse noise nor preserves sharp edges of an image. Hence, fuzzy filters with membership functions in terms of moving average and median center are taken into consideration for further processing.

In addition, Laws' mask method has achieved favourable acceptance in texture classification, still no attempts have been made to design a noise-robust Laws' mask descriptor. Hence, to extend the traditional Laws' mask descriptor towards noise robustness, in this paper, we focus on designing a hybrid model that includes the existing fuzzy filters and the traditional Laws' mask for noise texture analysis. The four fuzzy filters utilized in the proposed method are TMED, ATMED, TMAV and ATMV [15]. To validate the efficiency of the proposed descriptor on noisy dataset, two comprehensive texture databases are used in the experiments. As random noise (Gaussian) is more challenging type of noise compared to impulse noise (salt and pepper). Therefore, Gaussian noise is added to the images of the texture databases to evaluate the noise-robustness of the Laws' mask descriptor. The purpose of the proposed method is to reduce the Gaussian noise by combining the fuzzy filters with Laws' mask descriptor. Initially noisy images are generated by corrupting with Gaussian noise of different standard deviation values for Brodatz and STex databases. Then these corrupted images are transformed into fuzzy images by utilizing TMED, ATMED, TMAV and ATMV fuzzy filters. In the next step, these fuzzy images are convolved with Laws' mask descriptor and texture features are extracted. In the classification task, k-NN classifier is used.

The steps followed for implementation of integrated fuzzy filters with Laws' mask are described as below.

1) Take noise free texture images, convert it into gray scale and subimages. Afterwards the subimages are embedded with Gaussian noise of different values.
2) The noisy images are passed with four fuzzy filters of different window size and fuzzy transformed images are obtained.
3) The texture features are extracted with two approaches. In the first approach, the original Laws' mask is utilized for the extraction of texture features of the noisy images. In the second approach, original Laws' mask is utilized for the extraction of texture features of the fuzzy transformed images.
4) Classification is performed through k-NN classifier.

The proposed method is compared with the traditional Laws' mask method with the noisy and noise free databases. Excellent experimental results demonstrate that the proposed feature extraction technique is able to retain the finer details of the denoised images and improves the texture classification rates.

The paper is arranged as follows. The traditional Laws' mask descriptor and fuzzy filters are briefly reviewed in Section 2. Section 3 explains the proposed noise-robust Laws' mask descriptor in detail. The experimental setup and results are presented in Section 4. In Section 5 final conclusion is given.

2. Review of fuzzy filters and Laws' masks method

2.1. Fuzzy filters

In 2002, Kwan and Cai have defined fuzzy filter and from which they have derived seven different types of fuzzy filters [14]. If $x(m,n)$ is input of a two dimensional fuzzy filter, then the output of fuzzy filter is defined as follows.

$$y(m,n)=\frac{\sum_{(p,q)\in M}F[x(m+p,n+q)]\cdot x(m+p,n+q)}{\sum_{(p,q)\in M}F[x(m+p,n+q)]} \tag{1}$$

where $F[x(m,n)]$ is the window function and M is the area of the window. They have derived the fuzzy filter with symmetrical triangular with median center (TMED), the fuzzy filter with asymmetrical triangular with median center (ATMED), the fuzzy filter with triangular function with moving average center (TMAV) and the fuzzy filter with asymmetrical triangular function with moving average center (ATMV) by considering different window functions.

2.1.1. TMED

The fuzzy filter with a triangular function and the median value within a window with the center value defined as follows.

$$F[x(m+p,n+q)]=\begin{cases}1-[|x(m+p,n+q)-x_{med}(m,n)|]/x_{mm}(m,n)\\ for\ |x(m+p,n+q)-x_{med}(m,n)|\le x_{mm}(m,n)\\ 1\ for\ x_{mm}=0\end{cases} \tag{2}$$

$$x_{mm}(m,n)=max[x_{max}(m,n)-x_{med}(m,n),x_{med}(m,n)-x_{min}(m,n)] \tag{3}$$

where $x_{max}(m,n)$, $x_{min}(m,n)$, and $x_{med}(m,n)$ are, the maximum value, the minimum value and the median value respectively, for all the input values $x(m+p,n+q)$ for n, q ∈ M within the window M at discrete indexes(m,n).

2.1.2. ATMED

The fuzzy filter with an asymmetrical triangular function and the median value within a window with the center value defined as follows.

$$F[x(m+p,n+q)] = \begin{cases} 1-[|x_{med}(m,n)-x(m+p,n+q)|]/[x_{med}(m,n)-x_{min}(m,n)] \\ \quad for\ x_{min}(m,n) \le x(m+p,n+q) \le x_{med}(m,n) \\ 1-[|x(m+p,n+q)-x_{med}(m,n)|]/x_{max}(m,n)-x_{med}(m,n) \\ \quad for\ x_{med}(m,n) \le x(m+p,n+q) \le x_{max}(m,n) \\ 1\ for\ x_{med}(m,n)-x_{min}(m,n)=0 or x_{max}(m,n)-x_{med}(m,n)=0 \end{cases} \tag{4}$$

Here the degree of asymmetry depends on the difference between $x_{med}(m,n)-x_{min}(m,n)$ and $x_{max}(m,n)-x_{med}(m,n)$. $x_{max}(m,n)$, $x_{min}(m,n)$ and $x_{med}(m,n)$ represent the maximum value, the minimum value, and the median value of all the input values$x(m+p,n+q)$ for n, q ∈ M within the window M at discrete indexes(m,n).

2.1.3. TMAV

The symmetrical triangular fuzzy filter with the moving average value within a window chosen as its center value expressed as

$$F[x(m+p,n+q)] = \begin{cases} 1-[|x(m+p,n+q)-x_{mav}(m,n)|]/x_{mv}(m,n) \\ for\ |x(m+p,n+q)-x_{mav}(m,n)| \le x_{mv}(m,n) \\ 1\ for\ x_{mv}=0 \end{cases} \tag{5}$$

$$x_{mv}(m,n) = max[x_{max}(m,n)-x_{mav}(m,n), x_{mav}(m,n)-x_{min}(m,n)] \tag{6}$$

$x_{max}(m,n)$, $x_{min}(m,n)$ and $x_{mav}(m,n)$ represent the maximum value, the minimum value, and the moving average value of all the input values $x(m+p,n+q)$ for within the window M at discrete indexes(m,n).

2.1.4. ATMAV

The asymmetrical triangular fuzzy filter with the moving average value within a window chosen as the center value expressed as

$$F[x(m+p,n+q)] = \begin{cases} 1-[|x_{mav}(m,n)-x(m+p,n+q)|]/[x_{mav}(m,n)-x_{min}(m,n)] \\ \quad for\ x_{min}(m,n) \le x(m+p,n+q) \le x_{mav}(m,n) \\ 1-[|x(m+p,n+q)-x_{mav}(m,n)|]/x_{max}(m,n)-x_{mav}(m,n) \\ \quad for\ x_{mav}(m,n) \le x(m+p,n+q) \le x_{max}(m,n) \\ 1\ for\ x_{mav}(m,n)-x_{min}(m,n)=0 or x_{max}(m,n)-x_{mav}(m,n)=0 \end{cases} \tag{7}$$

The degree of asymmetry depends on the difference between $x_{mav}(m,n)-x_{min}(m,n)$ and $x_{max}(m,n)-x_{mav}(m,n)$. $x_{max}(m,n)$, $x_{min}(m,n)$ and $x_{mav}(m,n)$ represent the maximum value, the minimum value, and the moving average value of all the input values$x(m+p,n+q)$ for within the window M at discrete indexes (m,n).

2.2. Laws' masks method

In 1980, Kenneth Ivan Laws has suggested an approach for the extraction of texture features that describes texture properties such as regularity, uniformity, density, roughness etc., by utilizing a set of filters [2]. Originally he has recommended 1 × 3 vectors such as L3 = [1,2,1] for averaging, E3 = [−1, 0, 1] for edges and S3 = [−1, 2, −1] for spots. One-dimensional vectors are convolved in turn transposes with themselves or each other that create 1 × 5 vectors with a mnemonics Level, Edge, Spot, Wave, and Ripple as given below.

$$Level \rightarrow L5 = [1, 4, 6, 4, 1] = L3 * L3$$
$$Spot \rightarrow S5 = [-1, 0, 2, 0, -1] = -E3 * E3 = L3 * S3$$
$$Ripple \rightarrow R5 = [1, -4, 6, -4, 1] = S3 * S3$$
$$Edge \rightarrow E5 = [-1, -2, 0, 2, 1] = L3 * E3$$
$$Wave \rightarrow W5 = [-1, 2, 0, -2, 1] = -E3 * S3$$

where * symbolizes the convolution operation. Different two-dimensional convolution masks of 25 numbers can be generated by the convolution of each vertical vector with a horizontal one. These two-dimensional masks are known as Laws' masks that are convolved with texture image and subsequently energy metrics of the texture image are obtained.

3. Proposed methodology

This section details the proposed descriptor, whose principles are presented on the block diagram illustrated on Fig. 1. The fuzzy filters are capable of suppressing the noise but the edges are not preserved. On the other hand, in the set of Laws' mask one mask is particularly known for edge preservation. Therefore, it is suggested to integrate the edge preserving abilities of Laws' mask and noise reducing abilities of fuzzy filters to preserve the edge and to reduce the Gaussian noise simultaneously. Fuzzy membership function with either median or moving average center is estimated asymmetrically or symmetrically.

The proposed fuzzy filters based Laws' mask method is conducted in three steps: (1) the texture images are artificially embed-

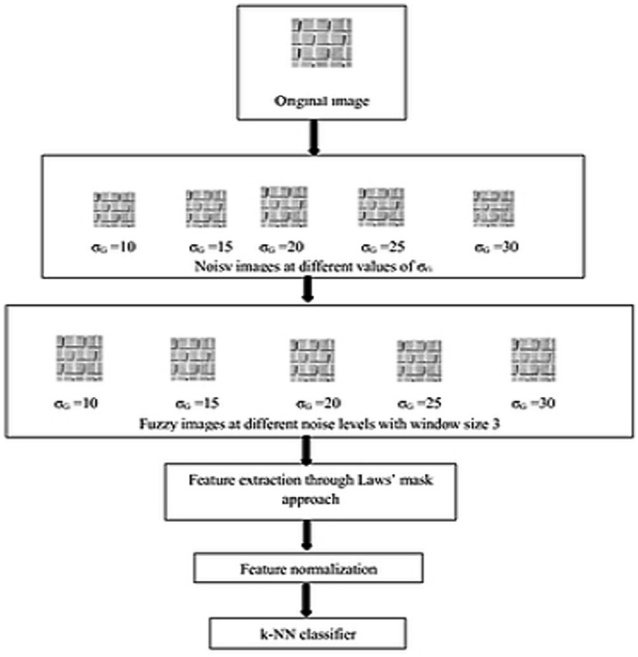

Fig. 1. Block diagram of the proposed method.

ded with Gaussian noise, (2) fuzzy filtering, and (3) feature extraction through Laws' mask descriptor.

1. Gaussian noise: The noise parameter contains Gaussian noise standard deviation (σ_G). The texture images are artificially embedded with Gaussian noise of different values and noisy images are obtained.
2. Fuzzy filtering: To extend the Laws' mask descriptor towards noise-robustness, fuzzy approach is applied. In the experiments four different types of fuzzy filter, namely, TMED, ATMED, TMAV, and ATMAV are employed to generate fuzzy transformed images. Square windows of dimensions M × M pixels are utilized in the experiments. Windows of three different width values (M = 3, 5, 7) are employed for conducting the experiments. Apart from noise reduction, the interests of the fuzzy filtering steps are to preserve edges and image details.
3. Feature extraction through Laws' mask descriptor:

The convolutions of the resultant fuzzy images are carried out with Laws' mask approach. In our experiment, we have selected only four masks by excluding the wave mask. These vectors are combined in 15 different ways to perform the convolution with the fuzzy images, for example E5S5, L5E5, L5R5, etc. After a series of convolution with particular masks, the outputs are passed through texture energy measurement (TEM) filters. Some statistical descriptors with moving non-linear window operation are used as energy measurement filters, through which each pixel is substituted by comparing with its local neighborhood pixel. Three statistical descriptors such as mean, absolute mean and standard deviation are utilized texture energy measurement filters in the experiments. The mean energy filter is named as MEF, the absolute mean energy filter is named as AMEF, and the standard deviation energy filter is named as SDEF. Once the series of specific convolution with selected filter masks are completed then the convolved outputs are applied to three different types of texture energy measurement filters for the investigation of the texture property of every pixel [6]. The filters are defined as follows.

$$MEF = \frac{\sum_P Neighbouringpixels}{P} \tag{8}$$

$$AMEF = \frac{\sum_P abs(Neighbouringpixels)}{P} \tag{9}$$

$$SDEF = \sqrt{\frac{\sum_P (Neighbouringpixels - mean)^2}{P}} \tag{10}$$

where P denotes the window size.

The generated outputs from these three texture energy measurement filters are normalized using min max normalization technique. The textural parameters such as absolute mean (ABSM), mean square or energy (MS) and entropy are evaluated for each normalized feature vector as follows.

$$ABSM = \frac{1}{LM}\sum_{x=1}^{L}\sum_{y=1}^{M}|I(x,y)| \tag{11}$$

$$Mean\ Square\ (MS) = \frac{1}{LM}\sum_{x=1}^{L}\sum_{y=1}^{M}I^2(x,y) \tag{12}$$

$$Entropy = \frac{1}{LM}\sum_{x=1}^{L}\sum_{y=1}^{M}I(x,y)(-lnI(x,y)) \tag{13}$$

where $I(x,y)$ is the pixel value, and L and M are the dimensions of image. Finally, to evaluate the efficiency of the suggested approach classification is performed using k-nearest neighbour classifier.

4. Experimental setup and result discussions

In this section, the feasibility of the proposed technique will be examined and the results are compared with the original Laws' mask descriptor. To demonstrate the performance of the proposed technique three different experiments are carried out on two benchmark databases: Brodatz and STex.

The Brodatz dataset is a very old and challenging platform for classification, presentation and analysis due to the exciting multiplicity and perceptual similarity of some textures [32]. In this database, some textures belong to the same class but at different scales, while others are so inhomogeneous that a human observer may be unable to group their samples correctly. Based on these considerations we have chosen the Brodatz dataset from which 24 numbers of image of size 640 × 640 pixels have been selected randomly as shown in Fig. 2. Splitting of each image into 25 non overlapping sub images of size 128 × 128 pixels. Thus, 600 patches are derived. Out of which 288 patches are utilized for training and 312 patches are utilized for testing.

The second dataset is collected from STex database that contains 476 different colour texture images of size 512 × 512 pixels [33]. The images are captured using three different cameras: Canon IXUS 70, Canon EOS 450D, and Nikon D40. For the analysis purpose, 25 different texture images are selected from this database as shown in Fig. 3. For this dataset also images are subdivided into sixteen 128 × 128 pixels non overlapping samples from which each 200 samples are used for traing and testing.

Experiment #1: Experiment #1 investigates the texture classification rates on grayscale images utilizing the traditional Laws' mask descriptor on both the datasets. Both the training and the testing images are convolved with fifteen numbers of masks. The convolved outputs are distributed over the three types of TEM filters of size 15x15, then the normalization is performed and texture features are evaluated. Thus each image produces 45 numbers of features. The classification results of the original Laws' mask descriptor are summarized in Table 1. The performance results of the two different datasets are shown in Fig. 4. It is observed that from three measurement filters the MEF has provided the classification rate of 93.27% on Brodatz dataset and 68.50% on STex dataset. The AMEF has provided classification rate of 86.22% on Brodatz dataset and 60.00% on STex dataset. The SDEF has delivered the classification rates of 89.42% and 61.00% on Brodatz and STex datasets respectively.

Experiment #2: Experiment #2 examines the texture classification rates on Gaussian noise corrupted images using the traditional

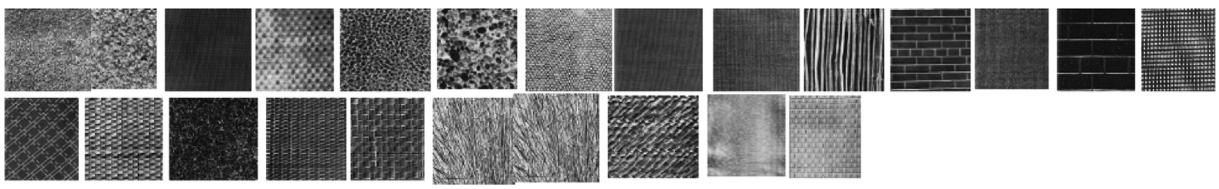

Fig. 2. 24 classes of Brodatz.

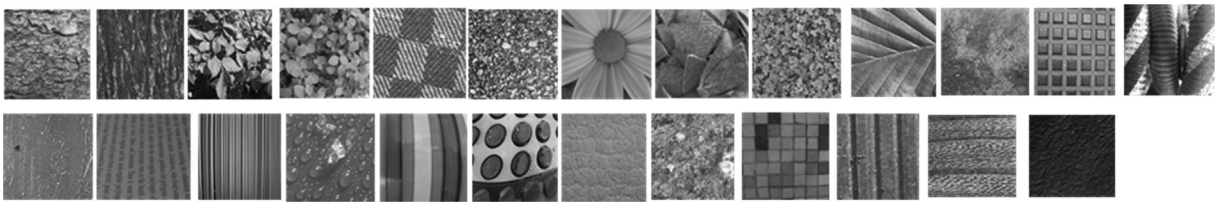

Fig. 3. 25 classes of STex.

Table 1
Results of the original Laws' mask approach on Brodatz and STex datasets.

Datasets used	Total number of features	Classification success rates (%)		
		MEF	AMEF	SDEF
Brodatz database				
masks used without wave	45	93.27	86.22	89.42
STex database				
masks used without wave	45	68.50	60.00	61.00

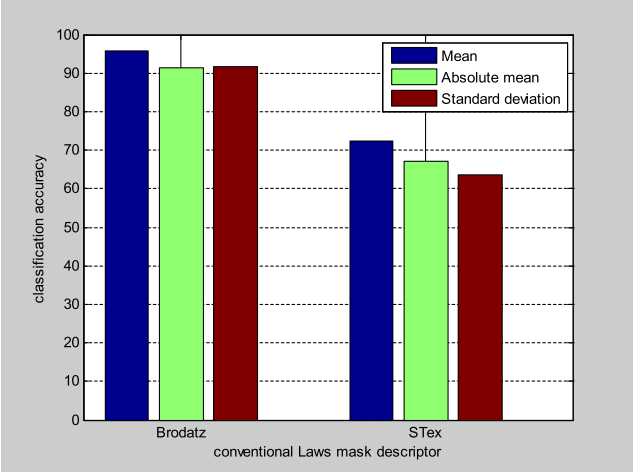

Fig. 4. Classification rates of traditional Laws' mask descriptor.

Laws' mask descriptor. Different levels of Gaussian noise standard deviation such as $\sigma_G = 10, 15, 20, 25, 30$ are chosen as the noise parameter values. The images are contaminated by adding the noise with different values as mentioned above for both the databases. For feature extraction, the same procedure is followed as described in the Experiment #1. Table 2 presents the classification rates of the noisy images on both the datasets. It is observed from the classification results that as the noise levels are increased accordingly the classification rates are decreased for all the three TEM filters. The results of noisy images at different noise levels on both databases are shown in Fig. 5 and Fig. 6.

Experiment #3: This experiment is carried out to investigate the robustness of the proposed scheme towards noised texture analysis using both the datasets. The images are corrupted by following the steps of Experiment #2. Then the corrupted images are passed through the TMED, ATMED, TMAV and ATMAV fuzzy filters to obtain fuzzy transformed images. The fuzzy transformed images are obtained using different windows of width values such as M = 3, 5, 7. The purpose of using different window values is to verify the effect of various noise levels at different window values. Next part of the experiment is to extract the texture features from fuzzy images through traditional Laws' mask descriptor. For features extraction the same procedure is followed as mentioned in

Table 2
Results of the traditional Laws' mask descriptor at different noise levels on both the datasets.

Approaches for texture parameter extraction	Total number of features	Classification Accuracy (%) for different noise level				
		$\sigma_G = 10$	$\sigma_G = 15$	$\sigma_G = 20$	$\sigma_G = 25$	$\sigma_G = 30$
Brodatz dataset						
MEF	45	92.31	91.03	89.42	88.70	87.18
AMEF	45	86.86	86.22	86.00	85.80	82.05
SDEF	45	88.78	87.82	87.42	86.54	81.09
STex dataset						
MEF	45	61.00	59.50	56.50	54.00	50.00
AMEF	45	59.50	51.50	48.50	40.00	36.00
SDEF	45	57.00	56.00	52.00	44.00	37.00

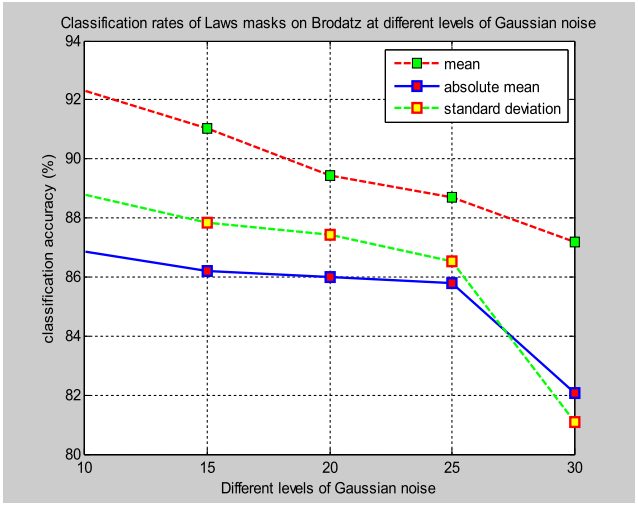

Fig. 5. Results of traditional Laws' mask for noisy images on Brodatz dataset.

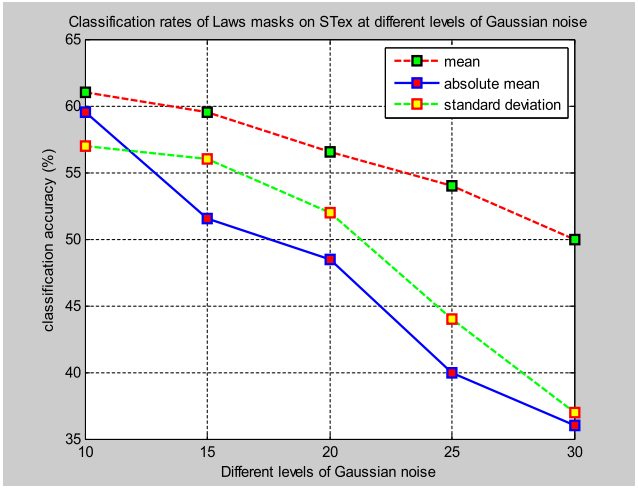

Fig. 6. Results of traditional Laws' mask for noisy images on STex dataset.

Experiment #1. The results of the different proposed methods on Brodatz and STex datasets are discussed separately as below.

4.1. Results on Brodatz dataset

Tables 3–6 represent the results of the proposed TMED, ATMED, TMAV, and ATMV fuzzy filter based Laws' mask method on Brodatz dataset.

Table 3 shows the classification success rates for the suggested TMED fuzzy filter based Laws' mask approach. The results displays that when $\sigma_G = 10$ maximum classification rate of 93.59% is achieved at M = 3 for the mean filter. When $\sigma_G = 15$ highest classification rate of 92.06% is obtained at M = 3 for the MEF. For the highly noisy images the improvement in classification accuracy occurred with higher window size i.e. when $\sigma_G = 20$ classification rate is 89.52% with M = 5, when $\sigma_G = 25$ classification rate is 89.10% at M = 7, and when $\sigma_G = 30$ classification rate is 89.26% at M = 7. However, for the AMEF there is not at all any improvement in classification rates are observed. For the SDEF higher classification rates are attained for only the window size M = 3. For the noise

Table 3
Results of the suggested **TMED** fuzzy Laws' mask approach on **Brodatz** dataset.

Approaches for texture parameter extraction	Total number of features	Classification Accuracy (%) for different noise level				
		$\sigma_G = 10$	$\sigma_G = 15$	$\sigma_G = 20$	$\sigma_G = 25$	$\sigma_G = 30$
MEF						
TMEDLaw (M = 3)	45	**93.59**	**90.06**	88.78	86.22	83.65
TMEDLaw (M = 5)	45	91.67	90.38	**89.52**	88.14	84.62
TMEDLaw (M = 7)	45	91.35	89.10	87.18	**89.10**	**89.26**
AMEF						
TMEDLaw (M = 3)	45	86.22	85.26	85.58	84.62	79.49
TMEDLaw (M = 5)	45	82.37	82.37	81.73	80.13	76.92
TMEDLaw (M = 7)	45	79.47	80.45	77.56	77.88	76.92
SDEF						
TMEDLaw (M = 3)	45	**90.71**	**88.78**	**92.31**	**87.50**	**84.94**
TMEDLaw (M = 5)	45	88.78	87.18	84.29	84.29	81.09
TMEDLaw (M = 7)	45	85.90	88.14	85.26	84.94	80.13

Table 4
Results of the suggested **ATMED** fuzzy Laws' mask approach on **Brodatz** dataset.

Approaches for texture parameter extraction	Total number of features	Classification Accuracy (%) for different noise level				
		$\sigma_G = 10$	$\sigma_G = 15$	$\sigma_G = 20$	$\sigma_G = 25$	$\sigma_G = 30$
MEF						
ATMEDLaw (M = 3)	45	**95.19**	**92.31**	**92.63**	**89.74**	**87.50**
ATMEDLaw (M = 5)	45	**92.63**	90.71	**91.67**	**89.42**	**89.74**
ATMEDLaw (M = 7)	45	89.74	88.46	86.86	85.26	87.18
AMEF						
ATMEDLaw (M = 3)	45	85.26	**88.14**	85.26	85.58	**82.69**
ATMEDLaw (M = 5)	45	81.73	81.09	77.24	83.97	81.41
ATMEDLaw (M = 7)	45	80.01	79.81	78.21	77.88	78.21
SDEF						
ATMEDLaw (M = 3)	45	**89.74**	**88.86**	**89.23**	**90.71**	**83.33**
ATMEDLaw (M = 5)	45	85.90	88.46	86.22	84.94	**83.33**
ATMEDLaw (M = 7)	45	82.05	81.09	81.64	80.13	**82.37**

Table 5
Results of the suggested **TMAV** fuzzy Laws' mask approach on **Brodatz** dataset.

Approaches for texture parameter extraction	Total number of features	Classification Accuracy (%) for different noise level				
		$\sigma_G = 10$	$\sigma_G = 15$	$\sigma_G = 20$	$\sigma_G = 25$	$\sigma_G = 30$
MEF						
TMAVLaw (M = 3)	45	**95.91**	**91.39**	**91.03**	88.46	84.62
TMAVLaw (M = 5)	45	92.05	90.71	**92.95**	**91.67**	**88.46**
TMAVLaw (M = 7)	45	**93.91**	**92.31**	**90.71**	**88.88**	**88.14**
AMEF						
TMAVLaw (M = 3)	45	**89.74**	**88.46**	**86.86**	**85.85**	80.13
TMAVLaw (M = 5)	45	**90.71**	**86.54**	**87.18**	79.17	79.17
TMAVLaw (M = 7)	45	**92.95**	**89.74**	**87.50**	**87.82**	**82.41**
SDEF						
TMAVLaw (M = 3)	45	**89.42**	**88.50**	**88.46**	**87.18**	81.09
TMAVLaw (M = 5)	45	**90.71**	**88.18**	**88.46**	**87.65**	**83.01**
TMAVLaw (M = 7)	45	**89.42**	**87.92**	**88.94**	**85.58**	**84.94**

Table 6
Results of the suggested **ATMAV** fuzzy Laws' mask approach on **Brodatz** dataset.

Approaches for texture parameter extraction	Total number of features	Classification Accuracy (%) for different noise level				
		$\sigma_G = 10$	$\sigma_G = 15$	$\sigma_G = 20$	$\sigma_G = 25$	$\sigma_G = 30$
MEF						
ATMAVLaw (M = 3)	45	**94.23**	**91.99**	**90.38**	**90.38**	**88.82**
ATMAVLaw (M = 5)	45	92.31	91.03	88.46	**89.10**	**88.14**
ATMAVLaw (M = 7)	45	88.14	85.90	87.82	**89.94**	**87.82**
AMEF						
ATMAVLaw (M = 3)	45	**89.13**	**87.76**	**88.18**	**88.78**	**84.62**
ATMAVLaw (M = 5)	45	86.54	85.58	85.58	**87.67**	**83.97**
ATMAVLaw (M = 7)	45	81.73	81.41	81.41	83.01	**83.65**
SDEF						
ATMAVLaw (M = 3)	45	86.54	87.82	**89.42**	**86.65**	**84.29**
ATMAVLaw (M = 5)	45	83.97	85.58	**87.50**	**87.82**	**84.62**
ATMAVLaw (M = 7)	45	82.69	82.05	83.01	**91.67**	**85.26**

Table 7
Results of the suggested **TMED** fuzzy Laws' mask approach on **STex** dataset.

Approaches for texture parameter extraction	Total number of features	Classification Accuracy (%) for different noise level				
		$\sigma_G = 10$	$\sigma_G = 15$	$\sigma_G = 20$	$\sigma_G = 25$	$\sigma_G = 30$
MEF						
TMEDLaw (M = 3)	45	**64.00**	**62.50**	52.00	47.00	47.00
TMEDLaw (M = 5)	45	**60.00**	**61.50**	54.00	51.50	48.00
TMEDLaw (M = 7)	45	58.00	58.00	56.50	53.00	48.50
AMEF						
TMEDLaw (M = 3)	45	52.00	47.00	40.50	37.50	31.00
TMEDLaw (M = 5)	45	50.50	44.50	40.50	40.00	35.00
TMEDLaw (M = 7)	45	47.00	46.50	46.50	**41.00**	**38.00**
SDEF						
TMEDLaw (M = 3)	45	57.00	50.00	44.00	39.50	31.00
TMEDLaw (M = 5)	45	46.50	45.50	39.00	38.00	38.50
TMEDLaw (M = 7)	45	50.50	49.00	42.50	**47.00**	**40.50**

Table 8
Results of the suggested **ATMED** fuzzy Laws' mask approach on **STex** dataset.

Approaches for texture parameter extraction	Total number of features	Classification Accuracy (%) for different noise level				
		$\sigma_G = 10$	$\sigma_G = 15$	$\sigma_G = 20$	$\sigma_G = 25$	$\sigma_G = 30$
MEF						
ATMEDLaw (M = 3)	45	**63.00**	**62.00**	**57.50**	**54.50**	**52.50**
ATMEDLaw (M = 5)	45	**60.00**	**61.00**	**57.00**	**58.50**	**58.50**
ATMEDLaw (M = 7)	45	**62.50**	58.50	58.50	58.00	53.50
AMEF						
ATMEDLaw (M = 3)	45	54.50	47.50	**49.50**	**42.00**	**39.50**
ATMEDLaw (M = 5)	45	50.50	47.00	**49.00**	**40.50**	**39.50**
ATMEDLaw (M = 7)	45	50.00	48.00	**49.00**	**51.00**	**43.50**
SDEF						
ATMEDLaw (M = 3)	45	52.50	48.00	**53.50**	**44.50**	**45.00**
ATMEDLaw (M = 5)	45	41.50	41.50	42.50	40.50	39.50
ATMEDLaw (M = 7)	45	42.50	46.00	43.00	**48.00**	**40.50**

Table 9
Results of the suggested **TMAV** fuzzy Laws' mask approach on **STex** dataset.

Approaches for texture parameter extraction	Total number of features	Classification Accuracy (%) for different noise level				
		$\sigma_G = 10$	$\sigma_G = 15$	$\sigma_G = 20$	$\sigma_G = 25$	$\sigma_G = 30$
MEF						
TMAVLaw (M = 3)	45	**62.50**	**59.53**	**57.50**	**54.50**	**52.00**
TMAVLaw (M = 5)	45	**63.00**	**62.50**	**57.50**	**55.50**	**56.50**
TMAVLaw (M = 7)	45	**64.50**	**62.00**	**61.00**	**57.50**	**53.00**
AMEF						
TMAVLaw (M = 3)	45	54.50	47.50	43.50	37.00	**37.50**
TMAVLaw (M = 5)	45	56.50	47.00	43.50	35.50	**42.50**
TMAVLaw (M = 7)	45	51.00	43.50	46.00	40.00	**43.00**
SDEF						
TMAVLaw (M = 3)	45	56.50	52.00	44.50	40.50	37.00
TMAVLaw (M = 5)	45	54.50	51.00	43.50	43.00	38.00
TMAVLaw (M = 7)	45	**59.00**	**57.00**	**53.00**	**49.00**	**39.50**

Table 10
Results of the suggested **ATMAV** fuzzy Laws' mask approach on **STex** dataset.

Approaches for texture parameter extraction	Total number of features	Classification Accuracy (%) for different noise level				
		$\sigma_G = 10$	$\sigma_G = 15$	$\sigma_G = 20$	$\sigma_G = 25$	$\sigma_G = 30$
MEF						
ATMAVLaw (M = 3)	45	**64.00**	**63.00**	**61.50**	**58.50**	**59.50**
ATMAVLaw (M = 5)	45	**62.00**	**63.50**	**58.50**	**59.50**	**57.50**
ATMAVLaw (M = 7)	45	**63.00**	**60.00**	**58.50**	**57.00**	**54.50**
AMEF						
ATMAVLaw (M = 3)	45	53.50	**52.50**	**49.00**	**47.50**	**42.00**
ATMAVLaw (M = 5)	45	50.50	**50.50**	**51.00**	**43.00**	**41.50**
ATMAVLaw (M = 7)	45	48.00	**53.00**	**54.00**	**50.00**	**42.00**
SDEF						
ATMAVLaw (M = 3)	45	48.00	53.50	46.50	44.00	41.00
ATMAVLaw (M = 5)	45	45.00	49.50	49.00	44.00	44.50
ATMAVLaw (M = 7)	45	45.50	45.00	**54.50**	**46.50**	**45.00**

levels $\sigma_G = 10$, $\sigma_G = 15$, $\sigma_G = 20$, $\sigma_G = 25$, and $\sigma_G = 30$ the corresponding classification accuracies achieved are of 90.71%, 88.78%, 92.31%, 87.50%, and 84.94% at M = 3 for the SDEF.

The classification success rates for the suggested ATMED fuzzy filter based Laws' mask approach are given in Table 4. From the table it is observed that the maximum classification accuracies for all the noise levels are attained for the window size M = 3. For the noise levels $\sigma_G = 10$, $\sigma_G = 15$, $\sigma_G = 20$, $\sigma_G = 25$, and $\sigma_G = 30$ the corresponding classification accuracies achieved are of 95.91%, 92.31%, 92.63%, 89.74%, and 87.50% at M = 3 for the

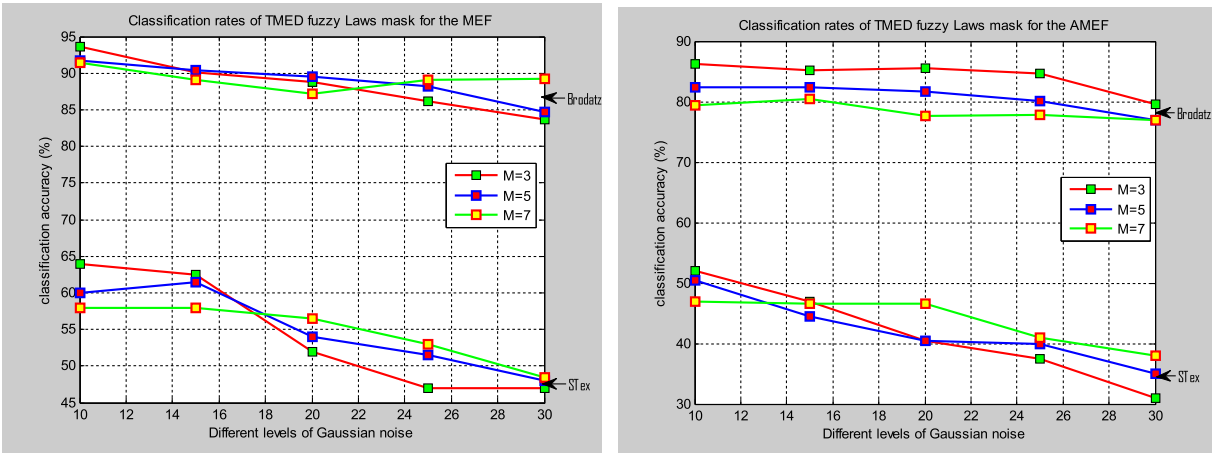

(a) (b)

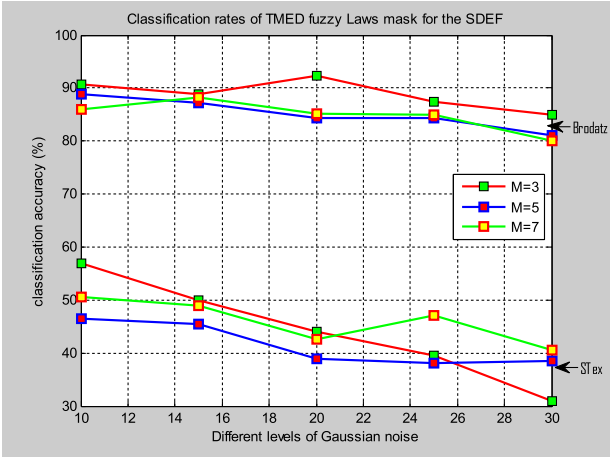

(c)

Fig. 7. Classification rates of TMED fuzzy filter based Laws' mask on both databases. (a) MEF (b) AMEF (c) SDEF.

MEF. Also for the window size M = 5 higher classification rates are noted for all the noise levels except $\sigma_G = 20$ for the MEF. For the AMEF higher classification rates are noted for only two noise levels i.e. 88.14% at $\sigma_G = 15$ and 82.69% at $\sigma_G = 30$. Similarly, for the SDEF increased classification rates are attained for the window size M = 3 at each level of noise. For the noise levels $\sigma_G = 10$, $\sigma_G = 15$, $\sigma_G = 20$, $\sigma_G = 25$, and $\sigma_G = 30$ the corresponding classification accuracies achieved are of 89.74%, 88.86%, 89.23%, 90.71%, and 83.33% at M = 3 for the SDEF.

The classification success rates for the suggested TMAV fuzzy filter based Laws' mask approach are given in Table 5. For this approach, maximum classification rates of 95.91%, 91.39%, and 91.03% are achieved when $\sigma_G = 10$, $\sigma_G = 15$, and $\sigma_G = 20$ respectively with M = 3 for MEF. As the noise levels are increased i.e. when $\sigma = 25$, and $\sigma = 30$ it is observed that there is no improvement in classification rates for the window size M = 3. For the higher noise levels such as $\sigma_G = 20$, $\sigma_G = 25$, the corresponding classification accuracies achieved are of 92.95%, 91.67%, and 88.46% with M = 5 for the MEF. Similarly with window size M = 7 for all the noise levels higher classification rates are attained for the MEF, i.e. for the noise levels $\sigma_G = 10$, $\sigma_G = 15$, $\sigma_G = 20$, $\sigma_G = 25$, and $\sigma_G = 30$ the corresponding classification rates are 93.91%, 91.39%, 90.71%, 88.88%, and 88.14%. For the AMEF the maximum classification accuracies are achieved continuously at window size M = 7 for all the noise levels. The classification rates of 92.95%, 89.74%, 87.50%, 87.82%, and 82.41% are attained when $\sigma_G = 10$, $\sigma_G = 15$, $\sigma_G = 20$, $\sigma_G = 25$, and $\sigma_G = 30$ respectively at M = 7 for the AMEF. However for window size M = 3 and M = 5 improvement in classification rates are noted for lower level of noise. Similarly for the SDEF the maximum classification accuracies are achieved for all the noise levels with window size M = 5 and M = 7. The classification rates of 90.71%, 88.18%, 88.46%, 87.65%, and 83.01% are attained when $\sigma_G = 10$, $\sigma_G = 15$, $\sigma_G = 20$, $\sigma_G = 25$, and $\sigma_G = 30$ respectively at M = 5 for the SDEF. The classification rates of 89.42%, 87.92%, 88.94%, 86.63%, and 84.94% are attained when $\sigma_G = 10$, $\sigma_G = 15$, $\sigma_G = 20$, $\sigma_G = 25$, and $\sigma_G = 30$ respectively at M = 7 for the SDEF. In addition higher classification rates are also obtained with window size M = 3 for lower noise levels for the SDEF.

The classification success rates for the suggested ATMAV fuzzy filter based Laws' mask approach are given in Table 6. For this approach, higher classification accuracies are attained for all the noise levels with window size M = 3 for the MEF. The classification rates of 94.23%, 91.99%, 90.78%, 90.38%, and 88.82% are attained when $\sigma_G = 10$, $\sigma_G = 15$, $\sigma_G = 20$, $\sigma_G = 25$, and $\sigma_G = 30$ respectively at M = 3 for the MEF. Classification rates are not improved for lower noise levels with window size M = 5 and M = 7 for the MEF. However, for the higher noise levels i.e. when $\sigma_G = 25$, and

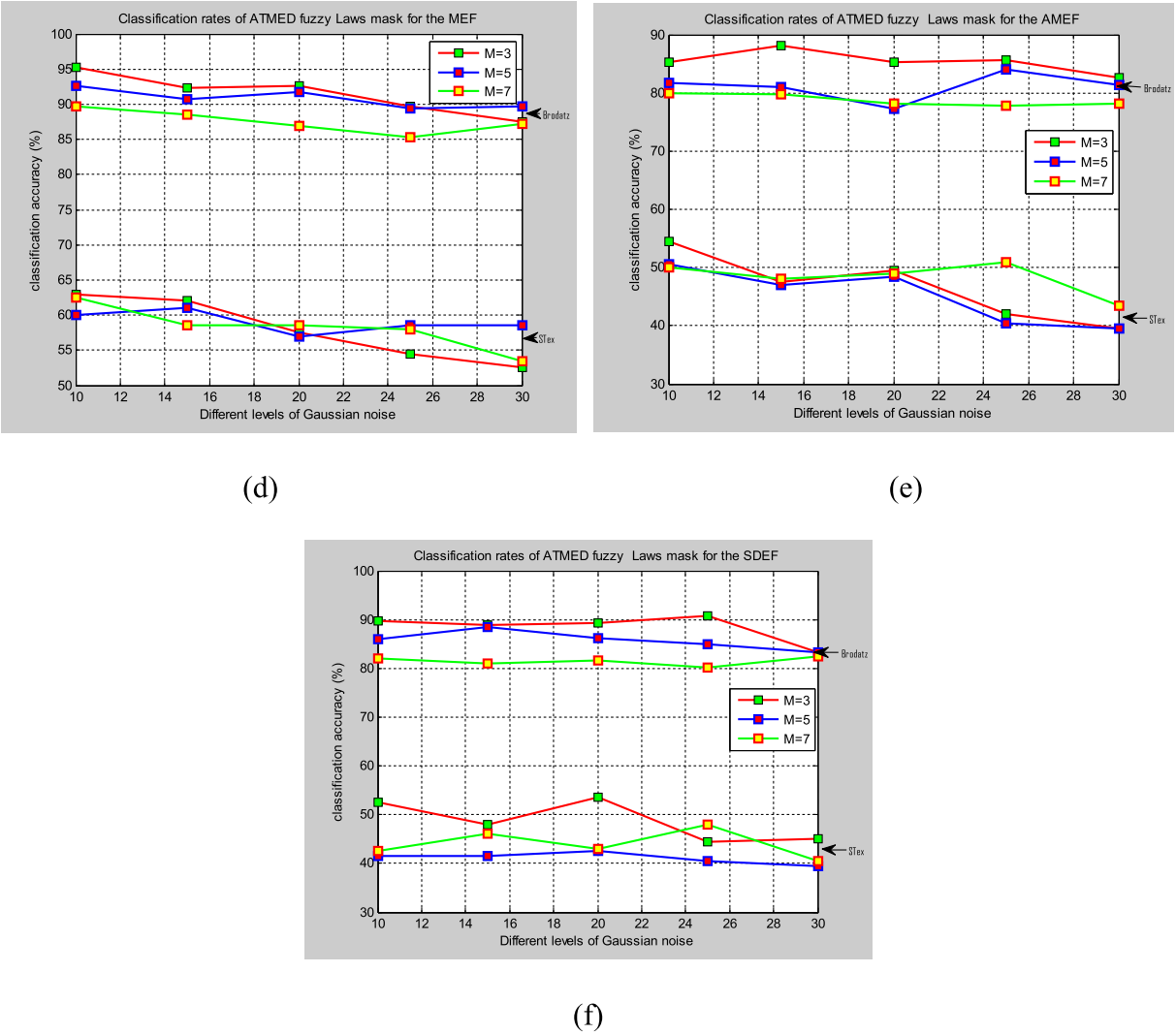

Fig. 8. Classification rates of ATMED fuzzy filter based Laws' mask on both databases. (d) MEF (e) AMEF (f) SDEF.

$\sigma_G = 30$ improved classification rates of 89.10%, 88.14% at M = 5, and 89.94%, 87.82% at M = 7 are obtained respectively for the MEF. Likewise for the AMEF higher classification accuracies of 89.13%, 87.76%, 88.18%, 88.78%, and 84.62% are achieved when $\sigma_G = 10$, $\sigma_G = 15$, $\sigma_G = 20$, $\sigma_G = 25$, and $\sigma_G = 30$ respectively at M = 3. Nevertheless, for the higher noise levels i.e. when $\sigma_G = 25$, and $\sigma_G = 30$ improved classification rates of 87.67%, 83.97% at M = 5, and when $\sigma_G = 30$ classification rate of 83.65% at M = 7 are obtained respectively for the AMEF. There is no increment in classification rates at the noise level $\sigma_G = 10$ and $\sigma_G = 15$for the SDEF by applying this technique. However it is observed that for the higher noise levels i.e. when $\sigma_G = 20$, $\sigma_G = 25$, and $\sigma_G = 30$ the classification accuracies are increased to 89.42%, 86.65%, and 84.29% at M = 3 and 87.50%, 87.82%, 84.62% at M = 5 respectively for the SDEF. For the window size M = 7 the classification accuracies are increased to 91.67% and 86.65% when $\sigma_G = 25$ and $\sigma_G = 30$ respectively for the SDEF.

4.2. Results on STex dataset

Tables 7–10 represent the results of the proposed TMED, ATMED, TMAV, and ATMV fuzzy filter based Laws' mask method on STex dataset.

The classification success rates for the suggested TMED fuzzy filter based Laws' mask approach are given in Table 7. For this approach, the classification accuracies are increased only for two noise levels with the window sizes i.e. M = 3 and M = 5 for the MEF. The classification rates of 64.00% and 62.50% for M = 3, and 60.00% and 61.50% for M = 5 are attained when $\sigma_G = 10$ and $\sigma_G = 20$ respectively for the MEF. For the rest of the noise levels classification accuracies are not improved by using any of the window sizes. Classification rates are not improved for lower noise levels for the AMEF using any of the window size. However, when $\sigma_G = 25$ and $\sigma_G = 30$ classification rates are improved to 41.00% and 38.00% at M = 7 for the AMEF. The similar case occurred in SDEF, when $\sigma_G = 25$ and $\sigma_G = 30$ classification rates are improved to 47.00% and 40.50% at M = 7.

The classification success rates for the suggested ATMED fuzzy filter based Laws' mask approach are given in Table 8. From the table it is observed that the maximum classification accuracies for all the noise levels are attained for the window sizes M = 3 and M = 5 for the MEF. For the noise levels $\sigma_G = 10$, $\sigma_G = 15$, $\sigma_G = 20$, $\sigma_G = 25$, and $\sigma_G = 30$ the corresponding classification accuracies achieved are of 63.00%, 62.00%, 57.50%, 54.50%, and 52.50% at M = 3, and 60.00%, 61.00%, 57.00%, 58.50%, and 58.50% at M = 5 for the MEF. For the window size M = 7 the higher classi-

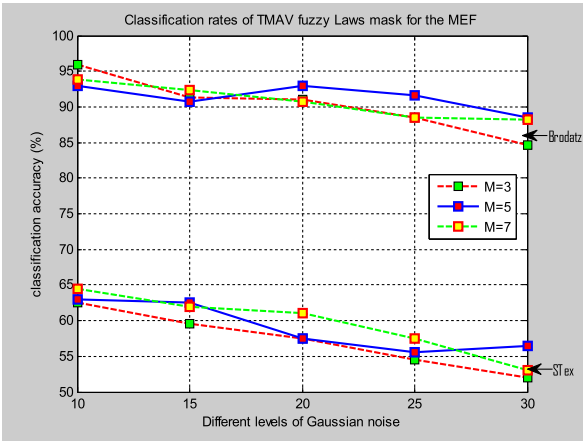

(g)

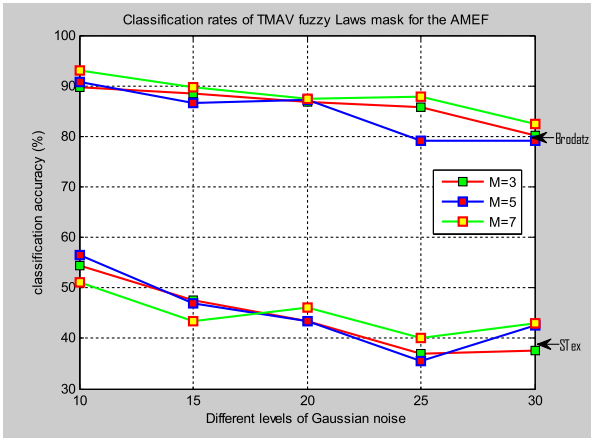

(h)

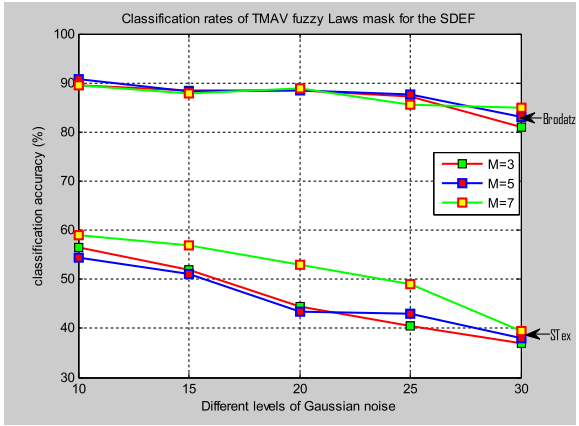

(i)

Fig. 9. Classification rates of TMAV fuzzy filter based Laws' mask on both databases. (g) MEF (h) AMEF (i) standard deviation filter.

fication rate of 62.50% is observed only when $\sigma_G = 10$ for the MEF. Classification rates are not improved for lower noise levels for the AMEF using any of the window size. However, when $\sigma_G = 20$, $\sigma_G = 25$ and $\sigma_G = 30$ classification rates are improved to 49.50%, 42.00%, and 39.50% at M = 3, 49.00%, 40.50%, and 39.50% at M = 5, and 49.00%, 51.00%, and 43.50% at M = 7 respectively for the AMEF. The similar case observed for the SDEF. The maximum improvement in the classification rates are of 53.50%, 44.50%, and 45.00% when $\sigma_G = 20$, $\sigma_G = 25$ and $\sigma_G = 30$ respectively at M = 3 for the SDEF. There is no improvement in the classification rates for the window size M = 5 for any of the noise levels. For the window size M = 7 maximum improvement in the classification rates are of 48.00% and 40.00% when $\sigma_G = 25$ and $\sigma_G = 30$ respectively For the SDEF.

The classification success rates for the suggested TMAV fuzzy filter based Laws' mask approach are given in Table 9. For this approach, higher classification accuracies are attained for all the noise levels with the entire window sizes i.e. M = 3, M = 5, and M = 7 for the MEF. The classification rates of 62.50%, 59.53%, 57.50%, 54.50%, and 52.00% are attained for all the noisy images at M = 3 for the MEF. The classification rates of 63.00%, 62.50%, 57.50%, 55.50%, and 56.50% are attained for all the noisy images at M = 5 for the MEF. The classification rates of 64.50%, 62.00%, 61.00%, 57.50%, and 53.00% are attained for all the noisy images at M = 7 for the MEF. For the AMEF, classification rates are not improved for lower noise levels using any of the window size. However, when $\sigma_G = 30$ classification rates increased to 37.50%, 42.50%, and 43.00% at window size M = 3, M = 5, and M = 7 respectively for the AMEF. For the SDEF the classification rates are not increased for any of the noisy images at window size M = 3 and M = 5. Yet the classification rates are increased to 59.00%, 57.00%, 53.00%, 49.00%, and 39.50% when $\sigma_G = 10$, $\sigma_G = 15$, $\sigma_G = 20$, $\sigma_G = 25$, and $\sigma_G = 30$ respectively at M = 7 for the SDEF.

The classification success rates for the suggested ATMAV fuzzy filter based Laws' mask approach are given in Table 10. Likewise in the previous approach in this approach also higher classification accuracies are attained for all the noise levels with the entire window sizes i.e. M = 3, M = 5, and M = 7 for the MEF. The classification rates of 64.00%, 63.00%, 61.50%, 58.50%, and 59.50% are attained for all the noisy images at M = 3 for the MEF. The classification rates of 62.00%, 63.50%, 58.50%, 59.50%, and 57.50% are attained for all the noisy images at M = 5 for the MEF. The classification rates of 63.00%, 60.00%, 58.50%, 57.00%, and 54.50% are attained for all the noisy images at M = 7 for the MEF. For the AMEF, classification rates are not improved for any of the window size when $\sigma_G = 10$. Yet when $\sigma_G = 15$, $\sigma_G = 20$, $\sigma_G = 25$, and $\sigma_G = 30$ classification rates are increased to 52.50%, 49.00%, 47.50%, and 42.00% at M = 3, 50.50%, 51.00%, 43.00%, and 41.50% at M = 5, and 53.00%, 54.00%, 50.00%, and 42.00% at M = 7 respectively for the AMEF. For the SDEF, classification rates are not improved for any of the noisy

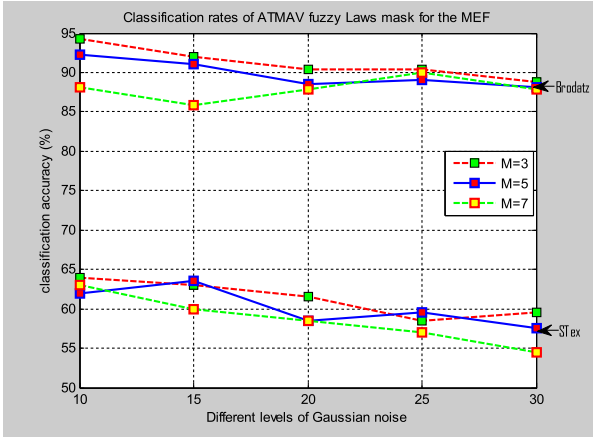

(j)

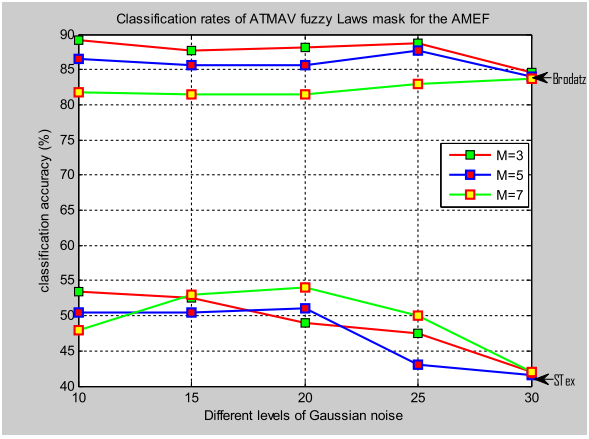

(k)

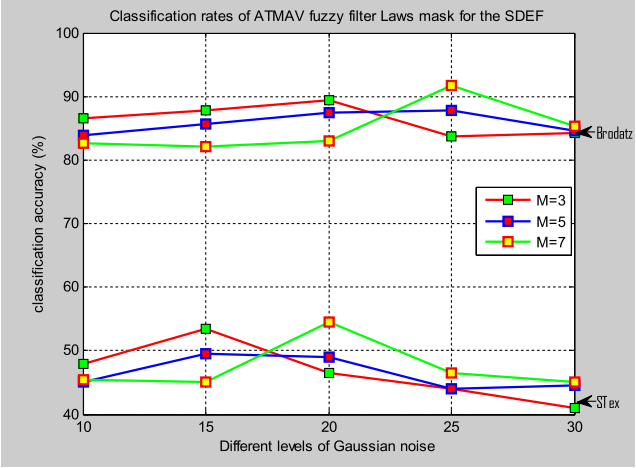

(l)

Fig. 10. Classification rates of ATMAV fuzzy filter based Laws' mask on both databases. (j) MEF (k) AMEF (l) SDEF.

Table 11
Classification results are compared with the suggested approaches and other state-of-the-art of texture classification methods.

Approach	Sample size (px) and Database	Noise Levels (σ)	Classification Accuracy (%)
Lee et al. [18]	64 × 64 (Brodatz)	–	97.5
Lakovidis et al. [21]	Thyroid Ultrasound	–	84
Zhu et al. [22]	200 × 200 (CUReT)	$\sigma = 0$	92.69
Zhu et al. [22]	200 × 200 (CUReT)	$\sigma = 20$	83.23
Zhu et al. [22]	200 × 200 (CUReT)	$\sigma = 40$	71.63
Zhu et al. [22]	128 × 128 (Outex 10)	$\sigma = 0$	98.34
Zhu et al. [22]	128 × 128 (Outex 12 "h")	$\sigma = 0$	92.75
Zhu et al. [22]	128 × 128 (Outex 12 "t184")	$\sigma = 0$	93.56
Zhu et al. [22]	128 × 128 (Outex)	$\sigma = 20$	90.47
Zhu et al. [22]	128 × 128 (Outex 10)	$\sigma = 40$	78.47
Zhu et al. [22]	128 × 128 (Outex 12 "h")	$\sigma = 40$	72.54
Zhu et al. [22]	128 × 128 (Outex 12 "t184")	$\sigma = 40$	72.74
Liu et al. [23]	Outex_TC11n	$\sigma = 5$	90.8
Liu et al. [23]	Outex_TC23n	$\sigma = 5$	73.8
Guo et al. [34]	(Outex 12 "t184")	–	97
Guo et al. [34]	Outex 12 "h")	–	96.5
Qi et al. [35]	Brodatz	–	94 ((±0.7)
Qi et al. [35]	KTH-TIPS	–	96((±0.9)
Fathi and Naghsh-Nilchi [36]	Brodatz	$\sigma = 5$	59.2 (±5.8)
Fathi and Naghsh-Nilchi [36]	CUReT	$\sigma = 5$	45.3 (±6.8)
Kylberg and Sintorn [37]	213 × 213 (Brodatz)	$\sigma = 0$	93.9
Kylberg and Sintorn [37]	200 × 200[b] (KTH-TIPS2b)	$\sigma = 0$	94.8
Kylberg and Sintorn [37]	288 × 288 (Kylberg[a])	$\sigma = 0$	98
Kylberg and Sintorn [37]	272 × 272 (Mondial Marmi)	$\sigma = 0$	91.1
Kylberg and Sintorn [37]	640 × 480 UIUC	$\sigma = 0$	87.3
Kylberg and Sintorn [37]	41 × 41 Virus	$\sigma = 0$	47
Proposed method	128 × 128 (Brodatz) (STex)	$\sigma = 10$	93.59 64
TMEDLaw(MEF)		$\sigma = 10$	
Proposed method	128 × 128 (Brodatz) (STex)	$\sigma = 10$	86.22 41
TMEDLaw(AMEF)		$\sigma = 25$	
Proposed method	128 × 128 (Brodatz) (STex)	$\sigma = 10$	90.71 47
TMEDLaw(SDEF)		$\sigma = 25$	
Proposed method	128 × 128 (Brodatz) (STex)	$\sigma = 10$	95.19 63
ATMEDLaw(MEF)		$\sigma = 10$	
Proposed method	128 × 128 (Brodatz) (STex)	$\sigma = 15$	88.14 51
ATMEDLaw(AMEF)		$\sigma = 25$	
Proposed method	128 × 128 (Brodatz) (STex)	$\sigma = 10$	89.74 53.50
ATMEDLaw(SDEF)		$\sigma = 20$	
Proposed method	128 × 128 (Brodatz) (STex)	$\sigma = 10$	95.91 64.50
TMAVLaw(MEF)		$\sigma = 10$	
Proposed method	128 × 128 (Brodatz) (STex)	$\sigma = 10$	92.95 43
TMAVLaw(AMEF)		$\sigma = 30$	
Proposed method	128 × 128 (Brodatz) (STex)	$\sigma = 10$	90.71 59
TMAVLaw(SDEF)		$\sigma = 10$	
Proposed method	128 × 128 (Brodatz) (STex)	$\sigma = 10$	94.23 64
ATMAVLaw(MEF)		$\sigma = 10$	
Proposed method	128 × 128 (Brodatz) (STex)	$\sigma = 10$	89.1354
ATMAVLaw(AMEF)		$\sigma = 20$	
Proposed method	128 × 128 (Brodatz) (STex)	$\sigma = 25$	91.67
ATMAVLaw(SDEF)		$\sigma = 20$	54.50

images for the window size M = 3 and M = 5. However, classification rates are increased to 54.50%, 46.50% and 45.00% when $\sigma_G = 20$, $\sigma_G = 25$, and $\sigma_G = 30$ at M = 7.

These results firmly demonstrate the noise robustness of the proposed techniques. Among all the suggested approaches the best results are provided by TMAV fuzzy Laws' mask technique on Brodatz database and ATMAV fuzzy Laws' mask technique on STex database. Furthermore, it is observed that when the window width increases, the filtering capability also increases for the high-level noise. Hence, larger windows are produced better results for the heavier noise. Fig. 7 depicts the achievements of the proposed TMED fuzzy filter based Laws' mask method. Fig. 8 shows the achievements of the suggested ATMED fuzzy filter based Laws' mask method. Fig. 9 represents the achievements of the proposed TMAV fuzzy filter based Laws' mask method. Fig. 10 represents the achievements of the proposed ATMAV fuzzy filter based Laws' mask method.

The classification success rates of the suggested approaches are compared with state-of-the-art of texture classification methods: Lee et al. [18], Lakovidis et al. [21], Zhu et al. [22], Liu et al. [23], Guo et al. [34], Qi et al. [35], Fathi and Naghsh-Nilchi [36], and Kylberg and Sintorn [37]. Table 11 illustrates the performance of the

Table 12
List of abbreviations.

Abbreviation	Technique
AMEF	Absolute mean energy filter
ATMED	Asymmetrical triangular with median center
ATMV	Asymmetrical triangular function with moving average center
GLCM	Gray Level Co-occurrence Matrix
k-NN	k-Nearest Neighbor
LBP	Local binary pattern
MED	Median
MEF	Mean energy filter
MAV	Moving average
SDEF	Standard deviation energy filter
TMED	Triangular with median center
TMAV	Triangular moving average center
TEM	Texture energy measurement

proposed approaches against the above approaches on various databases including different sample sizes. In the above-mentioned papers there are different types of noise with different levels are reported. In the Table 11, classification accuracies achieved with only Gaussian noises are discussed. For the proposed approaches, only the highest classification accuracies obtained from different Gaussian noise levels are discussed.

The list of abbreviations is listed in Table 12.

5. Conclusion

In this paper, a new approach is presented combining the existing fuzzy filters and Laws' mask approaches to enhance the performance of conventional Laws' mask for noise robustness in texture classification. The results on two texture databases such as Brodatz and STex validate that the proposed methods are capable of reducing high level of Gaussian noise, at the same time preserving image details, edges and textures well. In addition, the performance of the proposed methods is superior compared to the traditional Laws' mask method in terms classification on noisy texture images.

The encouraging results inspire to investigate further the application of the suggested approaches in areas like biomedical image analysis and SAR image analysis.

References

[1] Haralick RM, Shanmugam K, Dinstein I. Textural features for image classification. IEEE Trans Syst Man Cyb 1973;3(6):610–21.
[2] Laws KI. Texture energy measures. Proc. Image Understanding Workshop 1979:47-51.
[3] Laws KI. Textured image segmentation, Image Processing Institute, Univ. of Southern California, Report 940 1980.
[4] Legesse FB, Medyukhina A, Heuke S, Popp J. Texture analysis and classification in coherent anti-strokes Raman scattering (CARS) microscopy images for automated detection of skin cancer. Comp Med Img and Grap 2015;43:36–43.
[5] Setiawan AS, Elysia, Wesley J, Purnama Y. Mammogram classification using Law's energy measure and neural network. Procd Comp Sc 2015;59:92–7.
[6] Heba AE. Statistical analysis of Law's masks texture features for cancer and water lung detection. Int J of Comp Sc 2013;10(6):196–202.
[7] Rachidi M, Marchadier A, Gadois C, Lespessailles E, Chappard C, Benhamou CL. Laws' masks descriptors applied to bone texture analysis: an innovative and discriminant tool in osteoporosis. Skel Rad 2008;37(06):541–8.
[8] Dash S, Jena UR. Texture classification using steerable pyramid based Laws' masks. J of Elec Syst and Inf Tech 2017;4:185–97.
[9] Dash S, Jena UR. Multi-resolution Laws' masks based texture classification. J App Res Tech 2018;15:571–82.
[10] Dash S, Senapati MR, Jena UR. K-NN based automated reasoning using bilateral filter based texture descriptor for computing texture classification. Egyp Inf J 2018;19:133–44.
[11] Dash S, Jena UR, Senapati MR. Homorphic normalization-based descriptors for texture classification. Arab J Sc Eng 2018;43(8):4303–13.
[12] Lee C-S, Kuo Y-H, Yu P-T. Weighted fuzzy mean filters for image processing. Fuzzy Sets Syst 1997;89:157–80.
[13] Lee C-S, Kuo Y-H. Fuzzy Techniques in Image Processing. New York: Springer-Verlag, Studies in Fuzziness and Soft Computing, ch. Adaptive fuzzy filter and its application to image enhancement 2000;52:172–193.
[14] Farbiz F, Menhaj MB. Fuzzy Techniques in Image Processing. New York: Springer-Verlag, Studies in Fuzziness and Soft Computing, ch. A fuzzy logic control based approach for image filtering 2000; 52: 194–221.
[15] Ville DVD, Nachtegael M, Weken DVD, Kerre EE, Philips W, Lemahieu I. Noise reduction by fuzzy image filtering. IEEE Trans on Fuz Syst 2003;11(4):429–36.
[16] Kwan HK, Cai Y. Fuzzy filters for image filtering. In proceedings of the 45th Midwest Symposium on Circuits and Systems (MWSCAS) 2002;3:III-672-675.
[17] Kwan HK. Fuzzy filters for noisy image filtering. IEEE Int Symp on Circt and Syst (ISCAS'03) 2003; IV-161-164.
[18] Lee Y-G, Lee J-H, Hsueh Y-C. Texture classification using fuzzy uncertainty texture spectrum. Neurocomputing 1998;20:115–22.
[19] Ahonen T, Pietikainen M. Soft histograms for local binary Patterns. In Proc. Finnish Signal Proc Symp 2007; 645–649.
[20] Hoque N, Ahmed HA, Bhattacharyya DK, Kalita JK. A fuzzy mutual information-based feature selection method for classification. Fuz Infor Eng 2016;8:355–84.
[21] Lakovidis DK, Keramidas EG, Maroulis D. Fuzzy local binary patterns for ultrasound texture characterization. In: Camilho A, Kamel M, editors. Image analysis and recognition (lecture notes in computer science). Berlin, Germany: Springer; 2008. p. 750–9.
[22] Zhu Z, You X, Chen CLP, Tao D, Ou W, Jiang X, et al. An adaptive hybrid pattern for noise-robust texture analysis. Patt Recog 2015;48(8):2592–608.
[23] Liu L, Lao S, Fieguth PW, Guo Y, Wang X, Pietikainen M. Median robust extended local binary pattern for texture classification. IEEE Trans on Img Procs 2016;25(3):368–1138.
[24] Biradar N, Dewal ML, Rohit M. Speckle noise reduction using hybrid TMAV based fuzzy filter. Int J Resch Eng Tech 2014;3(3):113–8.
[25] Santoso AW, Pebrianti D, Lim TS, Bayuaji L, Latech H, Zain JM. Comparison of fuzzy filters on synthetic aperture radar image. In: 2nd international conference on science and technology-computer (ICST), Yogyakarta, Indonesia, 2016.
[26] Russo F, Ramponi G. A fuzzy filter for images corrupted by impulse noise. IEEE Sig Procs Lett 1996;3(6):168–70.
[27] Harron W, Dony R, Miller S. Noise reduction to enhance the classification of images using textural information. Canadian Conference on Elct and Comp Engg 2009;243-246.
[28] Schulte S, Witte VD, Nachtegael M, Weken DVD, Kerre EE. Fuzzy two-step filter for impulse noise reduction for color images. IEEE Trans Img Procs 2006;15(11):3567–78.
[29] Mehra M, Moraniya D, Nitnawwre D. Performance analysis of image de-noising using fuzzy and wiener filter in wavelet domain. Int J Comp App 2014;101(3):34–7.
[30] Bansal R, Sehgal P, Bedi P. A simplified fuzzy filter for impulse noise removal using thresholding. Procd of World Cong on Engg and Comp Sc (WCECS 2007) 2007.
[31] Toh KKV, Isa NAM. Noise adaptive fuzzy switching median filter for salt-and-pepper noise reduction. IEEE Sig Procs Lett 2010;17(3):281–4.
[32] Brodatz P. Textures: a photographic album for artists and designers. Dover & Greer Publishing Company; 1966.
[33] Department of Computer Sciences, U. S., Salzburg texture image database (STex) (www.wavelab.at/sources/stex), 2007.
[34] Guo Y, Zhao G, Pietikainen M. Discriminative features for texture description. Patt Recog 2012;45(10):3834–43.
[35] Qi X, Qiao Y, Li C, Guo J J. Multi-scale joint encoding of local binary patterns for texture and material classification. In Proc Brit Mach Vis Conf (BMVC), Sep 2013; 1-11.
[36] Fathi A, Naghsh-Nilchi AR. Noise tolerant local binary pattern operator for efficient texture analysis. Patt Recog 2012;33(09):1093–100.
[37] Kylberg G, Sintorn I-M. Evaluation of noise robustness for local binary pattern descriptors in texture classification. EURASIP J Img Vid Procss 2013;17:1–20.